Non-traditional stochastic models for ocean waves

Non-traditional stochastic models for ocean waves

Lagrange models and nested SPDE models

Georg Lindgren[1,a], David Bolin[1], and Finn Lindgren[1,2]

[1] Mathematical statistics, Lund University, Box 118, SE-221 00 Lund, Sweden
[2] Mathematical sciences, Norwegian University of Science and Technology, Trondheim, Norway

Abstract. We present two flexible stochastic models for 2D and 3D ocean waves with potential to reproduce severe and non-homogeneous sea conditions. The first family consists of generalized Lagrange models for the movements of individual water particles. These models can generate crest-trough and front-back statistically asymmetric waves, with the same degree of asymmetry as measured ocean waves. They are still in the Gaussian family and it is possible to calculate different slope distributions exactly from a wave energy spectrum. The second model is a random field model that is generated by a nested stochastic partial differential equation. This model can be adapted to spatially non-homogeneous sea conditions and it can approximate standard wave spectra. One advantage with this model is that Hilbert space approximations can be used to obtain computationally efficient representations with Markov-type properties that facilitate the use of sparse matrix techniques in simulation and estimation.

1 Introduction

The deterministic theory of ocean waves, formulated as a non-linear Schrödinger equation, has been shown to reproduce observed freak waves very accurately when properly calibrated. The equations are also successfully used to generate artificial freak waves, in a numeric or physical wave tank. Thus, physics, mathematics, and real ocean waves agree, at least in an ideal world, on an ocean without wind, breaking waves, foam, fixed offshore structures, sailing vessels, etc.

However, the deterministic, non-linear wave models in the form of non-linear partial differential equations, need for their solution boundary conditions, which are themselves waves. The models need also be calibrated against empirical data, in order to deliver useful numerical values for important wave characteristic properties. Furthermore, for simulation or computation purposes, they have to be parameterized from observable summary measures of the sea state, or other ocean weather conditions.

To model the inherent variability due to wind/wave interaction, and also to put some quantitative measure to the seemingly chaotic behavior of strongly non-linear waves, stochastic formulations are needed. The fully non-linear wave equations represent one extreme type of ocean wave models, and they are quite hard to put into a stochastic framework. The linear wave model, based on Fourier decomposition into elementary, independent, wave components, represents another extreme. It can easily be randomized, by letting elementary phases and amplitude be random, and in that form the linear Gaussian model has been used with great success since the early 1950's.

One reason for the popularity of the linear Gaussian model is that there is a direct connection between the correlation properties/power spectrum, and the statistical distributions,

[a] e-mail: georg.lindgren@matstat.lu.se

which is preserved under linear filtering. Another reason in the recent decades is the development of efficient computational tools for exact computation of important wave characteristic distributions, like wave amplitude and period distributions; see (14).

One obvious drawback of the Gaussian model is that it does not reproduce important wave characteristic distributions, in particular not in extreme cases. It gives statistically symmetric waves, both in the vertical, crest-trough, and in the horizontal, front-back, direction. To obtain statistical asymmetry, one has introduced higher order models, with interaction between frequency components, which deliver asymmetric waves, to the cost of a significant increase in computational complexity.

In this paper we present two alternatives to the linear Gaussian model for the water surface variability, which are more flexible and realistic, allowing asymmetric or non-homogeneous wave fields. The two models are a Lagrange model for the movements of individual water particles and a model formulated using a stochastic partial differential equation. The models still have enough Gaussian elements to make theoretical studies of important statistical distributions possible, and they can be used to through some light upon the problem of how extreme a wave has to be to be regarded as a freak wave, not belonging to the standard model.

The theory will be illustrated on a wave field with a standard Pierson-Moskowitz (PM) frequency spectrum with spectral density

$$S(\omega) = \frac{5H_s^2}{\omega_p(\omega/\omega_p)^5}\, e^{-\frac{5}{4}(\omega/\omega_p)^{-4}}, \quad 0 < \omega < \omega_c, \tag{1}$$

where $H_s = 4\sqrt{\mathsf{V}(W(t,u))}$ is the *significant wave height*, and ω_p is the *peak frequency*, and the *peak period* is defined as $T_p = 2\pi/\omega_p$. We use a fixed value $H_s = 7\,\mathrm{m}$ for the significant wave height, and assume a finite cut off frequency ω_c to obtain finite spectral moments and avoid small but high frequency wave components. For the nested SPDE model in Section 6, a directional spreading function

$$D(\theta) = c(\beta)\cos^{2\beta}(\theta - \theta_0) \tag{2}$$

is included in the spectrum.

2 The stochastic Lagrange wave model

The stochastic Lagrange wave model is a realistic alternative to the Gaussian linear model. Stochastic Lagrange models were introduced and studied by Gjøsund (8), Socquet-Juglard et al. (17), and Fouques et al. (7), who showed that Monte Carlo simulated stochastic Lagrange models can produce realistic crest-trough asymmetry as well as front-back asymmetry, the latter for higher order Lagrange models. Theoretical studies of their stochastic properties have recently been made by Lindgren and Åberg, (1; 2; 11; 12; 13). All these work deal with unidirectional waves and their space and time properties when observed along a fixed direction or fixed location in space.

2.1 The Gaussian wave field

To define the 3D Lagrange model, we let $W(t, \boldsymbol{s})$ be a Gaussian time varying random field with time parameter t and space parameter $\boldsymbol{s} = (u, v)$. In the Gaussian model, $W(t, \boldsymbol{s})$ would be the height of the water level at time t at location $\boldsymbol{s}$, but for the Lagrange model, we will use W as a model for water particle vertical movements.

The process $W(t, \boldsymbol{s})$ is a stochastic integral over wavenumber $\mathbf{k} = (k_1, k_2) \in \mathbb{R}^2$, or, alternatively over wave angular frequency $\omega > 0$ and wave direction $\theta \in (-\pi, \pi]$. Wave number and frequency/direction are assumed to be related via the depth dependent dispersion relation:

$$\omega = \omega(\mathbf{k}) = \sqrt{gk \tanh kh}, \qquad \theta = \arctan_2(k_2, k_1), \tag{3}$$

with the inverse $\mathbf{k} = \mathbf{k}(\omega, \theta) = (k_1, k_2)$, $k_1 = k\cos\theta$, $k_2 = k\sin\theta$, with $k = \|\mathbf{k}\| = \sqrt{k_1^2 + k_2^2}$, water depth h, and g denoting the earth gravitation constant. In (3), $\arctan_2$ is the four quadrant inverse tangent function.

We express the *real* Gaussian process as a stochastic integral of a *complex* spectral process, $\zeta(\mathbf{k}, \omega)$. To achieve this, we extend the wave number-frequency space from $(\mathbf{k}, \omega) \in \mathbb{R}^2 \times \mathbb{R}^+$ by allowing $(\mathbf{k}, \omega) \in \mathbb{R}^2 \times \mathbb{R}^-$, identifying a wave characterized by a certain set $(k_1, k_2; \omega, \theta)$ with a wave with characteristics $(-k_1, -k_2; -\omega, \theta + \pi \bmod 2\pi)$, reflecting (k_1, k_2, ω) in the origin.

Let $S_G(\omega, \theta), (\omega, \theta) \in \mathbb{R}^+ \times (-\pi, \pi]$, be the directional frequency spectrum of $W(t, \boldsymbol{s})$ and write

$$\widetilde{S_G}(\omega, \theta) = \begin{cases} \frac{1}{2}\, S_G(\omega, \theta)\, d\omega\, d\theta, & \text{if } \omega > 0, \\ \frac{1}{2}\, S_G(-\omega, \theta + \pi \bmod 2\pi), & \text{if } \omega < 0, \end{cases} \tag{4}$$

for the spectrum on the extended space $\mathbb{R} \times (-\pi, \pi]$. If one reflects (k_1, k_2, ω) in the origin one can define the spectral representation in a symmetric complex form. Writing

$$D = \left\{ (\mathbf{k}, \omega) \in \mathbb{R}^3; \omega = \pm\sqrt{gk \tanh kh} \right\},$$

for the dispersion surface, one has, with a small abuse of notation,

$$W(t, \boldsymbol{s}) = \int_{(\mathbf{k},\omega)\in D} e^{i(\mathbf{k}\boldsymbol{s} - \omega t)}\, d\zeta^K(\mathbf{k}, \omega) = \int_{\omega=-\infty}^{\infty} \int_{\theta=-\pi}^{\pi} e^{i(\mathbf{k}\boldsymbol{s} - \omega t)}\, d\zeta(\omega, \theta). \tag{5}$$

Here $\zeta^K(\mathbf{k}, \omega)$ is a Gaussian complex spectral process with mean 0 such that

$$d\zeta^K(-\mathbf{k}, -\omega) = \overline{d\zeta^K(\mathbf{k}, \omega)},$$

and $\zeta(\omega, \theta)$ the corresponding directional process with

$$d\zeta(-\omega, \theta) = \overline{d\zeta(\omega, \theta + \pi \bmod 2\pi)}.$$

2.2 The first order Lagrange wave model

2.2.1 The 3D model

The integral (5) defines the waves as a continuous version of a sum of independent cosine waves, with different directions and frequencies, and in the Gaussian model it gives the water level at location $\boldsymbol{s} = (x, y)$ at time t. The (first order) stochastic Lagrange model is built in a similar way, but instead of letting $W(t, \boldsymbol{s})$ be the height of the free water level at the fixed point (x, y), as in the Gaussian model, we let it describe the height of a water particle on the surface that at time t is located at $(X(t, \boldsymbol{s}), Y(t, \boldsymbol{s}))$, performing a random shift around $\boldsymbol{s} = (u, v)$, the *reference co-ordinate*. The physical interpretation of the model is that $(W(t, \boldsymbol{s}), X(t, \boldsymbol{s}), Y(t, \boldsymbol{s}))$ are the vertical and horizontal coordinates of an individual water particle on the surface.

The random shift processes, $(X(t, \boldsymbol{s}), Y(t, \boldsymbol{s}))$ are defined as a linear filtration of $W(t, \boldsymbol{s})$, depending on water depth h. To this end, specify a complex transfer function $\boldsymbol{H}(\theta, k)$, and define, integrating over $(\omega, \theta) \in \mathbb{R} \times (-\pi, \pi]$,

$$\boldsymbol{\Sigma}(t, \boldsymbol{s}) = \begin{pmatrix} X(t, \boldsymbol{s}) \\ Y(t, \boldsymbol{s}) \end{pmatrix} = \boldsymbol{s} + \int_\omega \int_\theta \boldsymbol{H}(\theta, \|\mathbf{k}\|)\, e^{i(\mathbf{k}\boldsymbol{s} - \omega t)}\, d\zeta(\omega, \theta). \tag{6}$$

The simplest form of the filtration is the *Miche filter*, where the transfer function, indexed by M, is (see (7; 8; 16)),

$$\boldsymbol{H}(\theta, k) = \boldsymbol{H}_M(\theta, k) = \begin{pmatrix} h_1(\theta, k) \\ h_2(\theta, k) \end{pmatrix} = i\, \frac{\cosh kh}{\sinh kh} \begin{pmatrix} \cos\theta \\ \sin\theta \end{pmatrix}, \quad \theta \in (-\pi, \pi], k > 0. \tag{7}$$

2.2.2 The 2D model

For unidirectional wave fields, parallel to the y-axis, one can use $X(t,(u,v)) = X(t,(u,0))$ and $Y(t,(u,v)) = v$. We call the model (7) the *free Lagrange model*. As we shall see, this model gives crest-trough asymmetric but front-back symmetric 2D waves. To generate also front-back asymmetry in 2D waves, one can introduce a more general transfer function, for example by the model

$$\frac{\partial^2 X(t,u)}{\partial t^2} = \frac{\partial^2 X_M(t,u)}{\partial t^2} - \alpha\, W(t,u), \tag{8}$$

with $\alpha > 0$. With $G(\omega) = -\frac{\alpha}{(-i\omega)^2}$ and the transfer function

$$H(\omega) = H_M(\omega) + G(\omega) = i\frac{\cosh kh}{\sinh kh} - \frac{\alpha}{(-i\omega)^2} = \rho(\omega)\, e^{i\,\theta(\omega)}, \text{ say,} \tag{9}$$

the horizontal movement process for uni-directional waves is expressed in the standard form,

$$X(t,u) = u + \int_{-\infty}^{\infty} e^{i(ku-\omega t+\theta(\omega))}\, \rho(\omega)\, d\zeta(\omega). \tag{10}$$

Comparing (10) with (6), we see that the free Lagrange model represents a phase shift between vertical and horizontal movement of $\theta = \pi/2 = 90^o$, while the general model has a *frequency dependent phase shift*, generating front-back asymmetry.

Definition 1 *(a) The first order 3D Lagrange model for ocean waves is the tri-variate Gaussian process* $(\boldsymbol{\Sigma}(t,\boldsymbol{s}), W(t,\boldsymbol{s}))$, $t \in \mathbb{R}$, $\boldsymbol{s} \in \mathbb{R}^2$.

(b) The first order 2D Lagrange model for uni-directional ocean waves is the bi-variate Gaussian process $(X(t,u), W(t,u))$, $t \in \mathbb{R}$, $u \in \mathbb{R}$.

Introduce the notations $W_t(t,u) = \partial W(t,u)/\partial t$, $X_u(t,u) = \frac{\partial X(t,u)}{\partial u}$, *etc, and write for the variances and covariances, for example,* $r^{ww} = \mathsf{V}(W(t,u))$, $r_{0t}^{ww} = \mathsf{Cov}(W(t,u), W_t(t,u))$, $r_{tu}^{wx} = \mathsf{Cov}(W_t(t,u), X_u(t,u))$, *etc.*

2.2.3 Space and time waves

The Lagrange model is constructed from the Gaussian surface by a random space deformation. The space wave field is obtained by keeping time constant $t = t_0$. A complication in the model is that folding may occur, leading to multiple values in some areas, i.e. $\boldsymbol{\Sigma}(t_0,\boldsymbol{s}_1) = \boldsymbol{\Sigma}(t_0,\boldsymbol{s}_2)$ with $\boldsymbol{s}_1 \neq \boldsymbol{s}_2$, and $W(t_0,\boldsymbol{s}_1) \neq W(t_0,\boldsymbol{s}_2)$.

The *space wave* field is defined implicitly by the relation

$$L(t_0, \boldsymbol{\Sigma}(t_0,\boldsymbol{s})) = W(t_0,\boldsymbol{s}), \tag{11}$$

and explicitly, if there is only one $\boldsymbol{s} = \boldsymbol{\Sigma}^{-1}(t_0,(x,y))$ satisfying $\boldsymbol{\Sigma}(t_0,\boldsymbol{s}) = (x,y)$, by

$$L(t_0,(x,y)) = W(t_0, \boldsymbol{\Sigma}^{-1}(t_0,(x,y))). \tag{12}$$

The *time wave* $L(t,(x_0,y_0))$ at a fixed location (x_0,y_0), is defined mathematically as the parametric curve

$$t \mapsto W(t, \boldsymbol{\Sigma}^{-1}(t,(x_0,y_0))), \tag{13}$$

provided the inverse $\boldsymbol{\Sigma}^{-1}(t,(x_0,y_0)) = \{\boldsymbol{s}; \boldsymbol{\Sigma}(t,\boldsymbol{s}) = (x_0,y_0)\}$ is uniquely defined at time t. Then there is only one water particle located at position (x_0,y_0) at time t. Otherwise, the Lagrangian time wave takes multiple values.

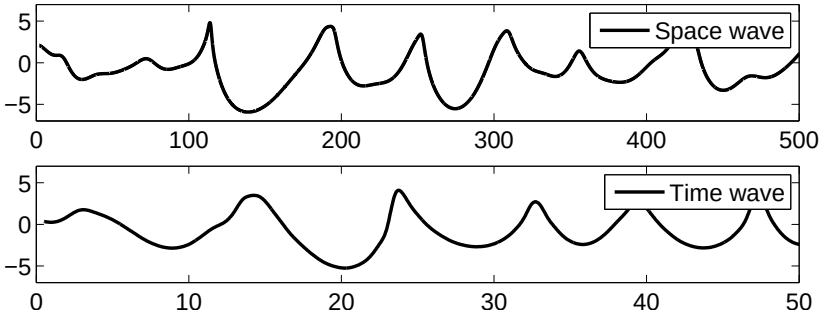

Fig. 1. Examples of asymmetric Lagrange space and time waves.

The spectral density $S(\omega, \theta)$ of the vertical process is called the *orbital spectrum*. Figure 1 shows examples of asymmetric 2D Lagrange space and time waves on extremely shallow water (to clearly show the asymmetry), and with $\alpha = 0.4$ in model (9). The orbital spectrum is uni-directional and is taken as a Pierson-Moskowitz (PM) spectrum (1).

From a shipping safety perspective, an intermediate type of wave record is most interesting, namely the *encountered waves*, the ones a ship meets during its voyage. Theoretically, these waves resemble the time waves, but with slightly modified spectra; see for example the overview by Åberg et al. (3).

3 Crest-trough asymmetry

3.1 Occupation density function for the Lagrangian wave

The statistical distribution of the Lagrangian space water level should describe how likely it is, at time t_0, to find a water particle at a specified height w at a specified location. For a spatially homogeneous random field we can without lack of generality take $(x_0, y_0) = (0, 0)$. We present the distribution for the 2D space waves, and consider the time wave at location $x_0 = 0$.

The folding phenomenon for Lagrangian space waves implies that one must define the statistical distribution of the level height as an *occupation density function*. We therefore introduce a notation for the number of particles that occupy a specific location, and also a notation for the number of such particles for which the height process fulfills some special condition.

Let $u \to (X(t_0, u), W(t_0, u)), u \in \mathbb{R}$, be a homogeneous parametric random curve, and write

$$N_x = \#\{u \in \mathbb{R} \text{ such that } X(t_0, u) = x\},$$
$$N_x(w) = \#\{u \in \mathbb{R} \text{ such that } X(t_0, u) = x \text{ and } W(t_0, u) \leq w\}.$$

The *occupation density* for the Lagrangian space process $(X(t_0, u), W(t_0, u))$ is a function $\mu(w), w \in \mathbb{R}$, such that, for every w_0, $\mathsf{E}(N_x(w_0)) = \int_{-\infty}^{w_0} \mu(w)\, dw$. If no folding can occur, then $\mathsf{P}(N_x > 1) = 1 - \mathsf{P}(N_x = 1) = 0$, and the occupation density is simply the probability density of the height of the water level observed in space, $\mathsf{P}(N_x(w) = 1) = \mathsf{E}(N_x(w))$.

The occupation density function for the Lagrangian space waves can easily be derived from Rice's formula for the expected number of level crossings by any non-stationary Gaussian process, and from its generalization to marked crossings; see (9). We formulate the results in a theorem, proved in (2), where $\phi(x)$ and $\Phi(x)$ denote the probability density and cumulative distribution function for the standardized normal distribution, and $\chi(A)$ stands for the indicator function for the event A.

Theorem 1 *a) For the stochastic Lagrangian space wave model, the expected number of particles occupying location x, and with height less than w_0 are, respectively,*

$$\begin{aligned}
\mathsf{E}(N_x) = \nu_0 &= \int_{-\infty}^{\infty} f_{X(0,u)}(0)\mathsf{E}\left(|X_u(0,u)| \mid X(0,u)=0\right)\, du \\
&= \mathsf{E}\left(|X_u(0,u)|\right) = 2\Phi\left(\frac{1}{\sqrt{r_{uu}^{xx}}}\right) - 1 + 2\sqrt{r_{uu}^{xx}}\,\phi\left(\frac{1}{\sqrt{r_{uu}^{xx}}}\right), \\
\mathsf{E}(N_x(w_0)) = \nu_0(w_0) &= \int_{-\infty}^{\infty} f_{X(0,u)}(0)\mathsf{E}\left(|X_u(0,u)|\,\chi_{W(0,u)\le w_0} \mid X(0,u)=0\right)\, du \\
&= \mathsf{E}\left(|X_u(0,u)|\,\chi_{W(0,u)\le w_0}\right) = \int_{-\infty}^{w_0} p_{W(0,u)}(w)\,\mathsf{E}(|X_u(0,u)| \mid W(0,u)=w)\, dw,
\end{aligned}$$

where $p_{W(0,u)}(w)$ is the normal probability density function of $W(0,u)$.

b) The conditional distribution of $X_u(0,u)$ given $W(0,u)=w$ is Gaussian with mean and variance given by

$$m(w) = 1 + w\,\frac{r_{0u}^{wx}}{r^{ww}}, \qquad \sigma^2_{x_u|w} = r_{uu}^{xx} - \frac{(r_{0u}^{wx})^2}{r^{ww}}. \tag{14}$$

c) The occupation density for the Lagrangian space wave is

$$\mu(w) = \frac{1}{\sqrt{2\pi r^{ww}}}\,\exp\left(-\frac{w^2}{2r^{ww}}\right) \times \left\{ m(w)\left(2\Phi\left(\frac{m(w)}{\sigma_{x_u|w}}\right) - 1\right) + \frac{2\sigma_{x_u|w}}{\sqrt{2\pi}} e^{-\frac{m(w)^2}{2\sigma^2_{x_u|w}}} \right\}. \tag{15}$$

The ratio $\nu_0(w)/\nu_0$ has the formal form of a cumulative distribution function, but due to the presence of multiple points it cannot be directly interpreted as such.

3.2 Example and practical conclusions

The Lagrangian space wave exhibits a crest-trough asymmetry, depending on water depth. We illustrate this effect and also draw some conclusions about the value of the significant wave height when it comes to evaluation of extreme wave height. For the orbital spectrum in the example we use the standard Pierson-Moskowitz, PM, spectrum, (1).

Figure 2 shows a histogram of observed occupations in a simulated Lagrangian space wave at (very) shallow water depth, $h = 4$m, compared to the theoretical occupation density (15). The figure is based on more than 65 000 sample points. The right diagram shows an enlargement of the extra intensity caused by the loops at high levels.

The severity of a sea state is usually characterized by the *significant wave height* $H_s = 4\,\sigma$, and the classification of a wave as a freak wave is therefore done in relation to the standard deviation σ of the sea surface. In Gaussian wave theory crest-to-trough wave heights rarely exceed twice the significant wave height, and waves above that height are therefore called freak or rogue waves, not belonging to the normal wave process. (The height limit for being regarded as a rough wave is of course chosen somewhat arbitrarily.) In the Lagrangian space model, the crest and trough heights are determined by the Gaussian vertical component $W(t_0,u)$ and the height of the local extremes are the same in the Gaussian and in the Lagrangian model. The standard deviation, however, will be lower after the X-deformation, leading to more waves being classified as extreme. In simulations we have found the following approximative ratios between the standard deviations in the Gaussian model with PM orbital spectrum and in the Lagrangian model, depending on water depth; Table 1.

The reduction is small but clear, and leads to the conclusion that some waves classified as rogue waves are in fact compatible with the model.

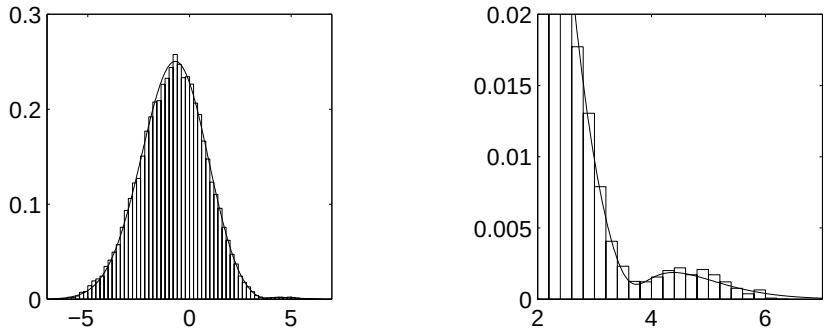

Fig. 2. Simulated Lagrangian space wave occupation distribution compared with the theoretical occupation density (15). Water depth $h = 4$m. Right diagram shows an enlargement of the upper part of the distribution. The simulation represents more than 16 000 m of space waves.

water depth	4m	8m	16m	32m	∞
$\frac{D(\text{Lagrangian})}{D(\text{Gaussian})}$	0.894	0.964	0.987	0.993	0.994

Table 1. Reduction of standard deviation D for the Lagrangian model as compared to the Gaussian model.

4 Space wave steepness

Severity of waves is not only a matter of wave height, but also of wave steepness. There are many definitions of wave steepness, and here we shall use a local definition of steepness, as the statistical distribution of the slope of the wave at its up- or downcrossings of a fixed level above or below the mean water level.

4.1 Asymmetry of the average wave

Figure 3 illustrates the asymmetry for different depths and degrees of asymmetry. The orbital spectrum is the PM spectrum with $H_s = 7$m and $T_p = 12$s. The solid curves give the average wave back shape centered around the upcrossing of the mean water level – which is negative due to the crest-trough asymmetry. The dash-dotted curves are the average of the steeper wave fronts, reversed to allow comparison with the wave backs. Each diagram is based on 1000 simulations of a Lagrange space wave $L(t_0, x)$, $0 \le x \le 2^{13}$, with sampling interval 0.5 m. Each curve is the average of more than 80 000 individual waves. The simulations were performed in the MATLAB toolbox WAFO; see (18).

4.2 Exact space wave slope distributions

The following exact slope distributions for the 2D Lagrange space waves were derived by Lindgren and Åberg (13). Due to the space distortion, the Lagrange waves exhibit in general steeper slopes than the Gaussian model at high level crossings, and the Lagrange model may therefore be a more suitable model for safety analysis of marine structures.

Consider the implicit definition (11) of the space wave at time t_0, $L(t_0, X(t_0, u)) = W(t_0, u)$. Then the slope of the space wave at the point $X(t_0, u)$ is the ratio $W_u(t_0, u)/X_u(t_0, u)$. This definition is unique if $X^{-1}(t_0, x)$ is uniquely defined; otherwise it defines a slope for each solution.

Now, each crossing of a fixed level w_0 by $W(t_0, u)$ as a function of u, corresponds to a crossing of the same level by the space wave. To find the slope distribution in the space wave

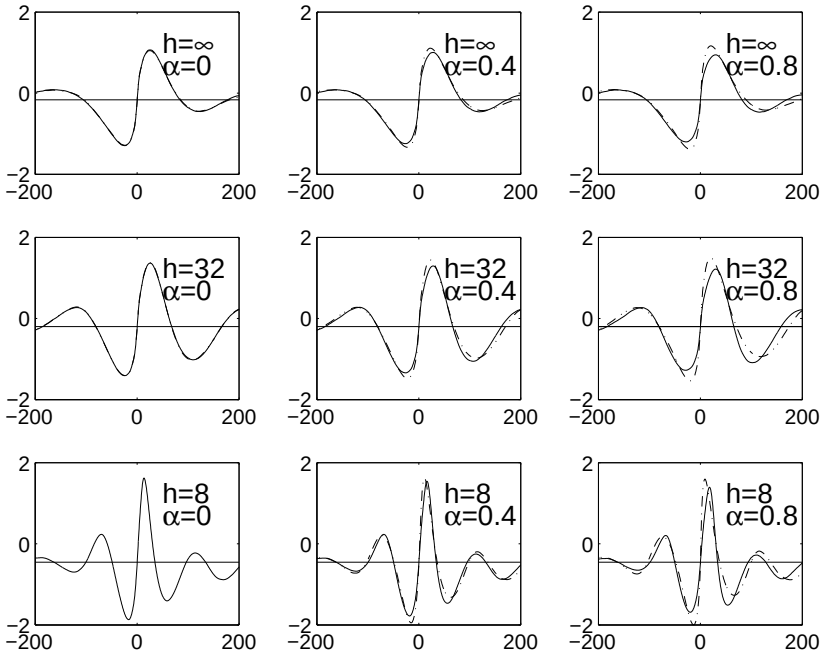

Fig. 3. Average up- and downcrossing waves. Solid curves = crest-back profiles, centered at mean level crossing; dash-dotted curves = reversed crest-front profiles, centered at downcrossings.

we therefore have to find the distribution of

$$L_x(t_0, X(t_0, u_k)) = \frac{W_u(t_0, u_k)}{X_u(t_0, u_k)}, \tag{16}$$

when u_k runs through all level w_0 crossings by $W(t_0, u)$, as a function of u.

From the definition, the distribution of the space wave slope at a crossing of the level w_0 is simply the distribution of the ratio (16) between the two dependent Gaussian derivatives, conditioned on the event that u_k is a w_0 crossing point in the vertical Gaussian process $W(t_0, u)$.

In the following theorem, R and U are two independent random variables, with probability densities, respectively,

$$f_R(r) = \frac{|r|}{2}\, e^{-r^2/2}, \text{ and } f_U(u) = \frac{1}{\sqrt{2\pi}}\, e^{-u^2/2},$$

i.e. R has a two-sided Rayleigh distribution and U is standard normal. The notation $X \stackrel{\mathcal{L}}{=} Y$ means that the random variables X and Y have the same distribution. Further, $r^{ww} = \mathsf{V}(W(t,u))$, $r^{wx}_{0u} = \mathsf{Cov}(W(t,u), X_u(t,u))$, etc.

Theorem 2 *The distribution of the space derivatives in* (16)*, under the condition that u_k is a v-crossing point in $W(t_0, u)$, can be expressed as*

$$W_u(t_0, u_k) \stackrel{\mathcal{L}}{=} R\sqrt{r^{ww}_{uu}},$$

$$X_u(t_0, u_k) \stackrel{\mathcal{L}}{=} 1 + v\,\frac{r^{wx}_{0u}}{r^{ww}} + R\frac{r^{wx}_{uu}}{\sqrt{r^{ww}_{uu}}} + U\sqrt{r^{xx}_{uu} - \frac{(r^{wx}_{0u})^2}{r^{ww}} - \frac{(r^{wx}_{uu})^2}{r^{ww}_{uu}}},$$

and hence, the slope $L_x(t_0, x_k)$, observed over all v-crossings, has the same distribution as

$$\frac{R\sqrt{r^{ww}_{uu}}}{1 + v\,\frac{r^{wx}_{0u}}{r^{ww}} + R\frac{r^{wx}_{uu}}{\sqrt{r^{ww}_{uu}}} + U\sqrt{r^{xx}_{uu} - \frac{(r^{wx}_{0u})^2}{r^{ww}} - \frac{(r^{wx}_{uu})^2}{r^{ww}_{uu}}}}. \tag{17}$$

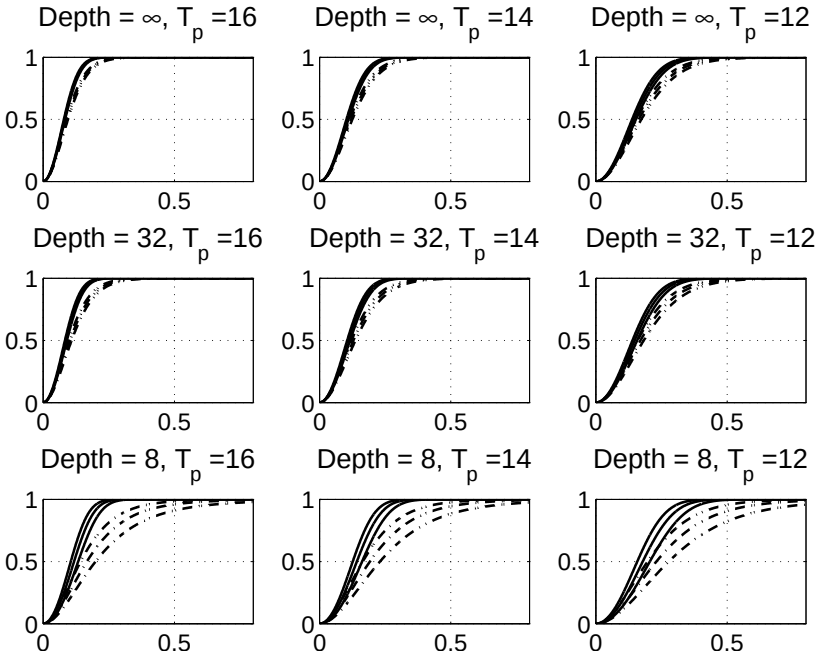

Fig. 4. Cumulative distribution functions for slopes in space at space wave upcrossings (solid lines) and negative slopes at downcrossings (dash-dotted lines) of levels -1, 0, 1 for Lagrange model (8) with $\alpha = 0.4$. Smallest slope at level -1, largest at +1.

The distributions at upcrossings or at downcrossings of the level v are obtained by replacing the two-sided Rayleigh variable by a one-sided, positive or negative, respectively. An explicit expression for the up- and downcrossing slope probability density function is given in (13).

A can be seen from (17) the covariance r_{uu}^{wx} is the crucial parameter for the front-back asymmetry. If it is zero, then slopes are statistically symmetric, while if it is non-zero up-crossing slopes and down-crossing slopes are statistically different. From the explicit formula

$$r_{uu}^{wx} = \mathsf{Cov}(W_u(t,u), X_u(t,u)) = \int_{-\infty}^{\infty} \kappa^2 \cos(\theta(\omega))\, \rho(\omega)\, S(\omega)\, d\omega,$$

one can see that it is the frequency dependent phase shift $\theta(\omega)$ that determines the degree of front-back asymmetry. Hence, it would be of interest to have empirical data on the correlation between the vertical and horizontal spatial gradients. Such data seems to be lacking at present.

The depth dependence of the front-back asymmetry for the Lagrange model (8) with PM orbital spectrum with different degrees of steepness ($T_p = 12, 14, 16$), and $\alpha = 0.4$ is illustrated in Figure 4. One can also see in the figure how the steepness increases with decreasing peak period.

5 Exact time wave properties

Time wave data, measured on a fixed point, are more abundant than space wave data. The time properties of the Lagrange model are somewhat more complicated to analyze from a statistical point of view than those of the space properties. We consider the 2D waves.

The Lagrange time waves satisfy, by definition, the relation $L(t, X(t,u)) = W(t,u)$. By differentiating with respect to t, we obtain

$$\frac{\partial L(t, X(t,u))}{\partial t} = W_t(t,u) = L_t(t, X(t,u)) + L_u(t, X(t,u))\, X_t(t,u).$$

By differentiating with respect to u, we obtain further, $W_u(t,u) = L_u(t,X(t,u))\,X_u(t,u)$, giving the fundamental definition of the time wave slope at location $X(t,u)$,

$$L_t(t,X(t,u)) = W_t(t,u) - W_u(t,u)\,\frac{X_t(t,u)}{X_u(t,u)}. \tag{18}$$

Equation (18) is a mathematical identity, and if $X^{-1}(t,x_0)$ is uniquely defined it also gives the unique slope of the Lagrange time wave $L(t,x_0)$ at location x_0. If there are multiple u-values such that $X(t,u) = x_0$, then we define $L_t(t,x_0)$ by (18) for each of these u-values.

To analyze crossings of a level w_0 in the 2D Lagrange time process, one has to identify, for a fixed location x_0, the instances t_k and reference points u_k where simultaneously $W(t_k,u_k) = w_0$, $X(t_k,u_k) = x_0$. Such bivariate crossing problems are extensively studied by Azaïs and Wschebor (4). The key instrument is the generalized Rice formula that gives the expected number of simultaneous solutions, unconditional as well as marked by some extra condition on an accompanying mark; see (12) for details.

We will illustrate the technique on two variables of interest in the safety analysis of fixed offshore structures, namely the derivative in time and the slope in space for a time wave that reaches a high level at a fixed location. Physical interpretations are the speed by which the water level rises and the steepness of the wall of water that may hit a deck of an offshore platform when the water level reaches a high level.

The slopes in space and time are defined by (16) and (18), respectively, and we seek their distribution at the times of the simultaneous occurrence of $W(t,X(t,u)) = w_0$ and $X(t,u) = x_0$.

Theorem 3 *The cumulative long run observable distribution function for time slope* (18) *at upcrossings of the level v in the Lagrange time wave, observed at location x_0, is given by,*

$$F_v^{TT+}(y) = \frac{1}{\mathsf{E}(N^+)} \int_{-\infty}^{\infty} g_y^{TT+}(u)\, f_{W(0,u),X(0,u)}(v,x_0)\, du, \tag{19}$$

where

$$\begin{aligned} g_y^{TT+}(u) &= \mathsf{E}\big(\big|W_t(0,u)X_u(0,u) - W_u(0,u)X_t(0,u)\big| \\ &\quad \times \mathbf{1}\big(0 < W_t(0,u) - W_u(0,u)\,\frac{X_t(0,u)}{X_u(0,u)} \le y\big) \;\big|\; W(0,u) = v, X(0,u) = x_0\big), \end{aligned} \tag{20}$$

$$\mathsf{E}(N^+) = \int_{-\infty}^{\infty} g_\infty^{TT+}(u)\, f_{W(0,u),X(0,u)}(v,x_0)\, du. \tag{21}$$

The cumulative distribution function of slopes at downcrossings is obtained by replacing the interval $(0,y]$ by the interval $[-y,0)$.

The distributions for space slope is found by replacing the event

$$\left\{0 < W_t(0,u) - W_u(0,u)\,\frac{X_t(0,u)}{X_u(0,u)} \le y\right\}$$

in (20) *by the event*

$$\left\{0 < W_t(0,u) - W_u(0,u)\,\frac{X_t(0,u)}{X_u(0,u)} \quad \textit{and} \quad W_u(0,u)/X_u(0,u) \le y\right\}.$$

Figures 5 and 6 show the cumulative distribution functions of the time and space slopes, respectively, observed at the instances when the time wave has an up- or downcrossing of a fixed level. Note that the space slopes at a time wave upcrossing are generally negative and they are positive when the time wave has a downcrossing.

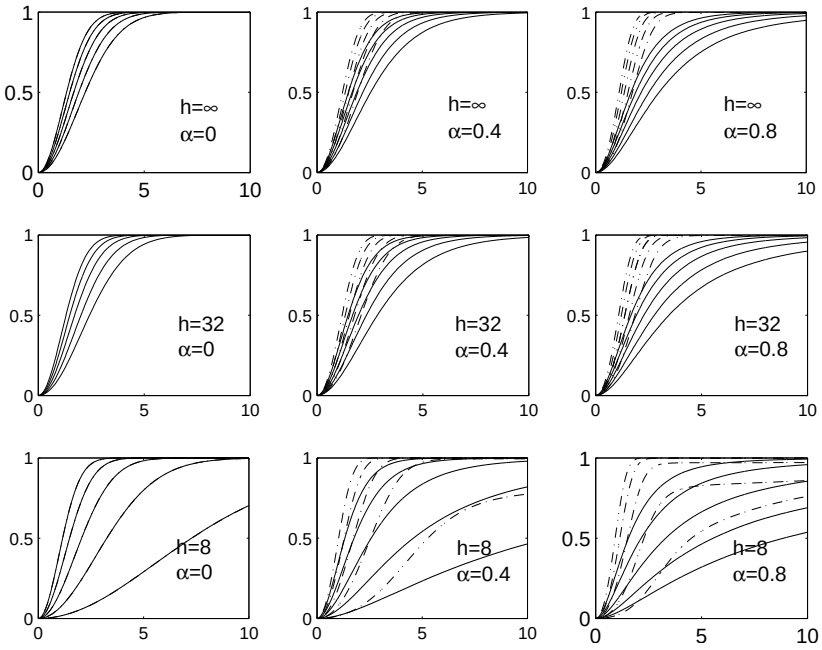

Fig. 5. Cumulative distribution functions for time wave slopes (absolute values) at time wave crossings of different levels. Slope CDF at upcrossings (solid lines) and at downcrossings (dash-dotted lines). Levels v: $[-1, 0, 1, 2, 3] \times \sigma$, $4\sigma = H_s$. Largest absolute values correspond to highest level. Orbital spectrum is PM.

6 Wave models using nested SPDEs

6.1 Nested SPDE approximation to classical wave models

The Lagrange model is based on Fourier analysis and it has a rather weak physical motivation. It is well suited to model statistically homogeneous fields, and it is not obvious how to modify it to spatially changing conditions. Recently, Bolin and Lindgren (6) derived a new class of random field models using nested stochastic partial differential equations (SPDE). This model is "local" and it can be calibrated to reproduce standard wave spectra.

The class of nested SPDE models is obtained by considering solutions to the SPDE

$$\left(\prod_{i=1}^{n_1}(\kappa_i^2 - \Delta)^{\frac{\alpha_i}{2}}\right) X(\mathbf{s}) = \left(\prod_{i=1}^{n_2}(b_i + \mathbf{B}_i^\top \nabla)\right) \mathcal{W}(\mathbf{s}). \tag{22}$$

Here, Δ is the Laplace operator, ∇ is the gradient, and $\mathcal{W}(\mathbf{s})$ is Gaussian white noise. The parameters in the SPDE are restricted such that $\alpha_i \in \mathbb{N}, \kappa_i^2 > 0, b_i \in \mathbb{R}$ and $\mathbf{B}_i \in \mathbb{R}^d$. The nested SPDE models is a wide family of stochastic fields for which many theoretical properties can be derived. Using basic linear filtering theory, the spectral density and covariance function for the solution, $X(\mathbf{s})$, to (22) can be obtained, and conditions for sample path continuity and sample path differentiability can also be found (6).

In what follows, we show how the standard wave model with a Pierson-Moskowitz wave-frequency spectrum and a cos-2s angular distribution (2) can be obtained as a limiting case from the class of nested SPDE models. In Equation (22), let the differential operators on the left hand side and right hand side be denoted by $\mathcal{L}_1$ and $\mathcal{L}_2$ respectively. A subclass of the nested SPDE models is considered by using $\mathcal{L}_1 = (\kappa^2 - \Delta)^{\frac{\alpha}{2}}$, and $\mathcal{L}_2 = (b + \mathbf{B}^\top \nabla)^\beta$, for some parameters $\kappa, b \in \mathbb{R}$, and $\mathbf{B} = (b_1, b_2)^\top \in \mathbb{R}^2$. Using Proposition 2.1 from (6), the wave number

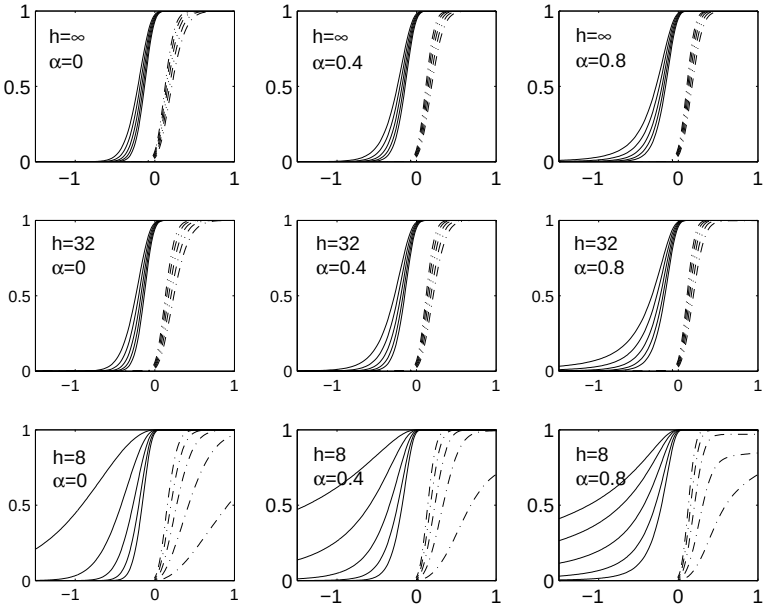

Fig. 6. Cumulative distribution functions for space wave slopes at time wave crossings of different levels. Slope CDF at upcrossings (solid lines) and at downcrossings (dash-dotted lines). Levels v: $[-1, 0, 1, 2, 3] \times \sigma$, $4\sigma = H_s$. Most extreme values correspond to highest level. Orbital spectrum is PM.

spectrum, denoted $R(\mathbf{k})$, for the resulting spatial field is

$$R(\mathbf{k}) = \frac{\phi^2}{(2\pi)^2} \frac{(b + \mathbf{k}^\top \mathbf{B}\mathbf{B}^\top \mathbf{k})^\beta}{(\kappa^2 + \mathbf{k}^\top \mathbf{k})^\alpha}.$$

By changing to polar coordinates such that $k_1 = k\cos(\theta)$ and $k_2 = k\sin(\theta)$, the wave number spectrum is related to the directional wave spectrum through

$$S(\omega, \theta) = R\left(k(\omega), \theta\right) \frac{\partial\, k(\omega)}{\partial\, \omega} k(\omega). \tag{23}$$

From the dispersion relation for the deep water case, one has $k = g^{-1}\,\omega^2$, where g is the gravitational acceleration. Using this expression in (23), one has

$$\begin{aligned} S(\omega, \theta) &= \frac{\phi^2}{(2\pi)^2} \frac{2\,\omega^3}{g^2} \frac{(b + \frac{\omega^4}{g^2}(b_1\cos(\theta) + b_2\sin(\theta))^2)^\beta}{(\kappa^2 + \frac{\omega^4}{g^2})^\alpha} \\ &= \frac{2\phi^2 g^{2\alpha}}{(2\pi)^2 g^2} \frac{\omega^3}{(g^2\kappa^2 + \omega^4)^\alpha} (b + \frac{\omega^4}{g^2}(b_1\cos(\theta) + b_2\sin(\theta))^2)^\beta \\ &= \frac{2\phi^2 g^{2\alpha}}{(2\pi)^2 g^2} \frac{\omega^3}{(g^2\kappa^2 + \omega^4)^\alpha} (b + \frac{\omega^4}{g^2}\cos^2(\theta - \theta_0))^\beta. \end{aligned}$$

Now, let $b = 0$, $\hat{\sigma}^2 = \phi^2 c(\beta)^{-1}$, and rearrange some of the terms to get

$$S(\omega, \theta) = \underbrace{\frac{2\hat{\sigma}^2 g^{2\alpha}}{(2\pi)^2 g^4} \frac{\omega^{4\beta+3}}{(g^2\kappa^2 + \omega^4)^\alpha}}_{S(\omega)} \underbrace{c(\beta)\cos^{2\beta}(\theta - \theta_0)}_{D(\theta)}$$

Thus, this is a directional spectrum with a cos-2s distribution as the angular dependent part and a wave frequency spectrum

$$S(\omega) = \frac{2\hat{\sigma}^2 g^{2\alpha}}{(2\pi)^2 g^4} \frac{\omega^{4\beta+3}}{(g^2\kappa^2 + \omega^4)^\alpha}.$$

Using $\beta = \alpha - 2$, $\kappa^2 = \frac{B_{PM}}{g^2\alpha}$, and $\hat{\sigma}^2 = \frac{A_{PM}(2\pi)^2 g^4}{2g^{2\alpha}}$, one has

$$S(\omega) = \frac{A_{PM}\,\omega^{4\alpha-5}}{(\frac{B_{PM}}{\alpha} + \omega^4)^\alpha} = \frac{A_{PM}}{\omega^5(\frac{B_{PM}}{\alpha\,\omega^4}+1)^\alpha} \to \frac{A_{PM}}{\omega^5} e^{-\frac{B_{PM}}{\omega^4}}, \text{ as } \alpha \to \infty.$$

Hence, by choosing the parameters as described above, the nested SPDE model converges to a wave model with a Pierson-Moskowitz wave frequency spectrum and a cos-2s angular distribution. Now, for $\beta = s$, the L_1-norm of the approximation error is

$$\int_0^\infty \left| \frac{A_{PM}}{\omega^5(\frac{B_{PM}}{\alpha\,\omega^4}+1)^\alpha} - \frac{A_{PM}}{\omega^5} e^{-\frac{B_{PM}}{\omega^4}} \right| \mathrm{d}\,\omega = \frac{A_{PM}}{5B_{PM}} \int_0^\infty \frac{1}{(\frac{x}{\alpha}+1)^\alpha} - e^{-x}\,\mathrm{d}x$$
$$= \frac{A_{PM}}{5B_{PM}} \left(\frac{\alpha}{\alpha - 1} - 1 \right) = \frac{A_{PM}}{5B_{PM}} \left(\frac{s+2}{s+1} - 1 \right) = \frac{A_{PM}}{5B_{PM}(s+1)},$$

where the variable transformation $x = B_{PM}\,\omega^{-4}$ was used in the first step. The results are summarized in the following proposition.

Proposition 1 *The spectral density for $X(\mathbf{s})$ given by the nested SPDE model*

$$\left(\frac{B_{PM} g^{-2}}{s+2} - \Delta \right)^{\frac{s+2}{2}} X(\mathbf{s}) = \left(\mathbf{B}^\top \nabla \right)^s \mathcal{W}(\mathbf{s})$$

converges to a random wave model with a Pierson-Moskowitz wave frequency spectrum and a cos-2s angular distribution $D(\theta) = c(s)\cos^{2s}(\theta - \theta_1)$ as $s \to \infty$. For a fixed s, the nested SPDE model has an exact cos-2s angular distribution and an error of $\frac{A_{PM}}{5B_{PM}(s+1)}$ in the wave frequency spectrum approximation measured in the L_1-norm.

The limitation is that the parameters in the cos-2s-distribution are connected to the order of the approximation, since $\alpha = s + 2$ is used. This should not be a big problem in practice since the convergence is reasonably fast. As shown in Figure 7, the wave frequency spectrum is similar to the Pierson-Moskowitz spectrum even for the worst case $s = 1$, and the difference for, the in practice common, case $s = 15$ will likely be smaller than the parameter estimation error if the model is fitted to data. If one is not satisfied with the approximation in the wave frequency spectrum for a given value of s, a closer fit can be obtained by changing $\hat{\sigma}$. Another way to obtain a better approximation is to use $\mathcal{L}_1 = \prod_{i=1}^{s+2}(\kappa_i^2 - \Delta)^{\frac{1}{2}}$. Figure 7 also shows the L_1-optimal approximations assuming that $\mathcal{L}_1$ is on the product form. An example of a realization of the SPDE model can be seen in Figure 8.

A last thing to note is that, since the nested SPDE models are purely spatial models, the angular dependent part is always symmetric in the sense that $D(\theta + \pi) = D(\theta)$. That is, one can obtain cos-2s distributions on the form $\cos^{2s}(\theta - \theta_0)$ but not on the form $\cos^{2s}(\frac{\theta - \theta_0}{2})$. The reason being that if the sea is observed only at a specific moment, one will not be able to determine if waves are going "forward" or "backward". To get around this problem, one would have to include time in the generating SPDE, and how this could be done is currently being investigated.

The nested SPDE representation of the Pierson-Moskowitz wave model has two main advantages. Firstly, since it is a local representation, non-stationary extentions are easy to obtain by spatially varying the parameters of the SPDE. Secondly, the nested SPDE formulation is valid on other domains than $\mathbb{R}^2$, and one can therefore use it for modeling waves on, for example, the sphere. Another advantage with the model is that Hilbert space approximations can be used to obtain computationally efficient representations of the model, as shown by Lindgren et al. (15). These representations have Markov-type properties that facilitate the use of efficient sparse matrix techniques in simulation and estimation of the model. We conclude this section with a brief introduction to these efficient representations.

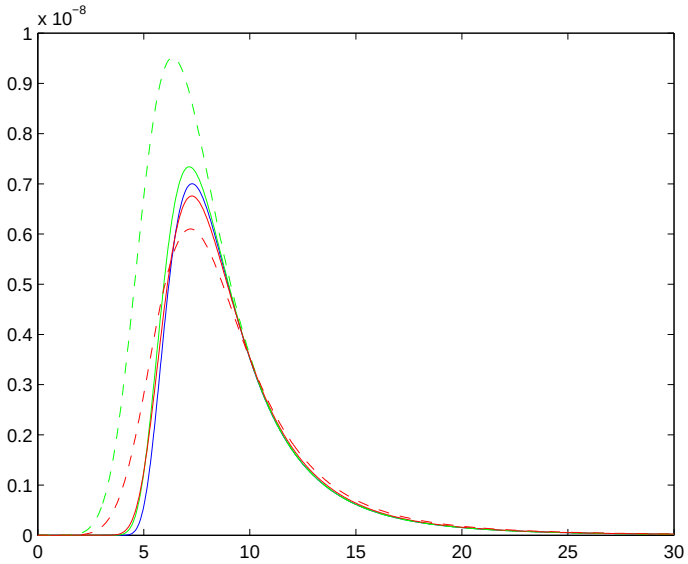

Fig. 7. A Pierson-Moskowitz wave frequency spectrum (blue curve) and approximations for the worst case $s = 1$ (dashed curves) and the common case $s = 15$ (solid curves). The green curves are the approximations from Proposition 1 and the red curves are L_1-optimal approximations for the given operator orders.

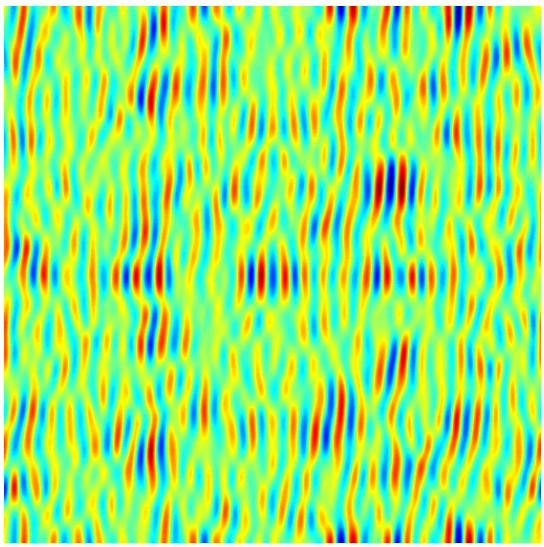

Fig. 8. Realization of the nested SPDE model in Proposition 1 with $s = 15$.

6.2 Computationally efficient representations

In this section, we give a brief introduction to the Hilbert space approximation technique by Lindgren et al. (15), and show how it can be extended to the class of nested SPDE models; see also the basic paper by Lindgren and Rue (10).

Lindgren et al. (15) derive a method for obtaining computationally efficient Markov representations of the, in environmental statistics, popular Gaussian Matérn fields. Their key idea is to approximate the solution to the SPDE $(\kappa^2 - \Delta)^{\frac{\alpha}{2}} X(\mathbf{s}) = \phi \mathcal{W}(\mathbf{s})$ in an approximation space Φ_n spanned by some basis functions $\varphi_1(\mathbf{s}), \ldots, \varphi_n(\mathbf{s})$. The weak solution of the SPDE with respect to the approximation space Φ_n can be written as $\tilde{x}(\mathbf{s}) = \sum_{i=1}^n w_i \varphi_i(\mathbf{s})$, where the stochastic weights $\{w_i\}_{i=1}^n$ are chosen such that the weak formulation of the SPDE is satisfied:

$$\left[\left\langle \varphi_i,\, (\kappa^2 - \Delta)^{\frac{\alpha}{2}} \tilde{x} \right\rangle_{\Omega}\right]_{i=1,\ldots,n} \overset{D}{=} \left[\langle \varphi_i,\, \mathcal{W} \rangle_{\Omega}\right]_{i=1,\ldots,n}. \tag{24}$$

Here $\overset{D}{=}$ denotes equality in distribution, Ω is the manifold on which $\mathbf{s}$ is defined, and $\langle f,\, g \rangle_{\Omega} = \int_{\Omega} f(\mathbf{s}) g(\mathbf{s})\, \mathrm{d}\mathbf{s}$ is the scalar product on Ω.

As an illustrative example, consider the first fundamental case $\alpha = 2$. With $\mathcal{L} = \kappa^2 - \Delta$, one has

$$\langle \varphi_i,\, \mathcal{L}\tilde{x} \rangle_{\Omega} = \sum_{j=1}^n w_j \langle \varphi_i,\, \mathcal{L}\varphi_j \rangle_{\Omega},$$

so by introducing the matrix $\mathbf{K}$, with elements $\mathbf{K}_{i,j} = \langle \varphi_i,\, \mathcal{L}\varphi_j \rangle_{\Omega}$, and the vector $\mathbf{w} = (w_1, \ldots, w_n)^\top$, the left hand side of (24) can be written as $\mathbf{K}\mathbf{w}$. Since

$$\langle \varphi_i,\, \mathcal{L}\varphi_j \rangle_{\Omega} = \kappa^2 \langle \varphi_i,\, \varphi_j \rangle_{\Omega} - \langle \varphi_i,\, \Delta\varphi_j \rangle_{\Omega} = \kappa^2 \langle \varphi_i,\, \varphi_j \rangle_{\Omega} + \langle \nabla\varphi_i,\, \nabla\varphi_j \rangle_{\Omega},$$

the matrix $\mathbf{K}$ can be written as $\mathbf{K} = \kappa^2\mathbf{C} + \mathbf{G}$ where $\mathbf{C}_{i,j} = \langle \varphi_i,\, \varphi_j \rangle_{\Omega}$ and $\mathbf{G}_{i,j} = \langle \nabla\varphi_i,\, \nabla\varphi_j \rangle_{\Omega}$. The right hand side of (24) can be shown to be Gaussian with mean zero and covariance $\mathbf{C}$. Thus, if $\mathbf{K}$ is invertible, one has

$$\mathbf{K}\mathbf{w} \sim \mathsf{N}(0, \mathbf{C}) \Leftrightarrow \mathbf{w} \sim \mathsf{N}(0, (\mathbf{K}^\top \mathbf{C}^{-1} \mathbf{K})^{-1}).$$

For the second fundamental case, $\alpha = 1$, it is shown in (15) that $\mathbf{w} \sim \mathsf{N}(0, \mathbf{K}^{-1})$. Given these two fundamental cases, the weak solution for any $\alpha \in \mathbb{N}$ can be obtained recursively. If, for example, $\alpha = 4$ the solution to $(\kappa^2 - \Delta)^2 X_0(\mathbf{s}) = \mathcal{W}(\mathbf{s})$ is obtained by solving $(\kappa^2 - \Delta) X_0(\mathbf{s}) = \tilde{x}(\mathbf{s})$, where $\tilde{x}$ is the weak solution for the case $\alpha = 2$.

The iterative way of constructing solutions can be extended to give us weak solutions to (22) as well. First, note that the SPDE $\mathcal{L}_1 X(\mathbf{s}) = \mathcal{L}_2 \mathcal{W}(\mathbf{s})$ can be written as the system of nested SPDEs

$$\begin{aligned} \mathcal{L}_1 X_0(\mathbf{s}) &= \mathcal{W}(\mathbf{s}), \\ X(\mathbf{s}) &= \mathcal{L}_2 X_0(\mathbf{s}). \end{aligned} \tag{25}$$

Let $\tilde{x}_0 = \sum_{i=1}^n w_i^0 \varphi_i(\mathbf{s})$ be a weak solution to $\mathcal{L}_1 X_0(\mathbf{s}) = \mathcal{W}(\mathbf{s})$, and let $\mathbf{Q}_{X_0}$ denote the precision for the weights $\mathbf{w}_0 = (w_1^0, \ldots, w_n^0)^\top$. Substituting X_0 with $\tilde{x}_0$ in the second equation of (25), the weak formulation of the equation is

$$[\langle \varphi_i,\, \tilde{x} \rangle_{\Omega}]_{i=1,\ldots,n} \overset{D}{=} [\langle \varphi_i,\, \mathcal{L}_2 \tilde{x}_0 \rangle_{\Omega}]_{i=1,\ldots,n} = \left[\sum_{j=1}^n w_j^0 \langle \varphi_i,\, \mathcal{L}_2 \varphi_j \rangle_{\Omega}\right]_{i=1,\ldots,n}. \tag{26}$$

First consider the case of an order-one operator $\mathcal{L}_2 = b_1 + \mathbf{B}_1^\top \nabla$. By introducing the matrix $\mathbf{H}_1$ with elements $\mathbf{H}_{1i,j} = \langle \varphi_i,\, \mathcal{L}_2 \varphi_j \rangle_{\Omega}$, the right hand side of (26) can be written as $\mathbf{H}_1 \mathbf{w}_0$. Introducing the vector $\mathbf{w} = (w_1, \ldots, w_n)^\top$, the left hand side of (26) can be written as $\mathbf{C}\mathbf{w}$, and one thus has

$$\mathbf{w} = \mathbf{C}^{-1}\mathbf{H}_1\mathbf{w}_0 \Rightarrow \mathbf{w} \sim \mathsf{N}(0, \mathbf{C}^{-1}\mathbf{H}_1\mathbf{Q}_{X_0}^{-1}\mathbf{H}_1^\top \mathbf{C}^{-\top}).$$

Now, if $\mathcal{L}_2$ is on the product form as in (22), the procedure can be used recursively, in the same way as when producing higher order Matérn fields. For example, if $\mathcal{L}_2 = (b_1 + \mathbf{B}_1^\top \nabla)(b_2 + \mathbf{B}_2^\top \nabla)$,

the solution is obtained by solving $X(\mathbf{s}) = (b_2 + \mathbf{B}_2^\top \nabla)\tilde{x}(\mathbf{s})$, where $\tilde{x}$ is the weak solution to the previous example. Thus, when $\mathcal{L}_2$ is on the product form, one has

$$\mathbf{w} \sim \mathsf{N}(0, \mathbf{H}\mathbf{Q}_{X_0}^{-1}\mathbf{H}^\top), \quad \mathbf{H} = \mathbf{C}^{-1}\mathbf{H}_{n_2}\mathbf{C}^{-1}\mathbf{H}_{n_2-1}\cdots\mathbf{C}^{-1}\mathbf{H}_1,$$

where each factor $\mathbf{H}_i$ corresponds to the $\mathbf{H}$-matrix obtained in the the i:th step in the recursion.

If the basis functions $\varphi_i(\mathbf{s})$ are orthogonal and have compact support, the matrices $\mathbf{Q}_{X_0}$ and $\mathbf{H}_i$ are sparse, and efficient sparse matrix techniques can be used for simulation and estimation. Thus, bases such as the Daubechies wavelets are suitable for these approximations (5). This approximation procedure can also be extended to the class of non-stationary nested SPDE models, and hence to non-stationary wave models specified through nested SPDEs. For details, see (6).

References

1. Aberg, S. (2007). Wave intensities and slopes in Lagrangian seas. *Adv. Appl. Prob.*, **39**, pp. 1020–1035.
2. Aberg, S. and Lindgren, G. (2008). Height distribution of stochastic Lagrange ocean waves. *Probabilistic Engineering Mechanics*, **23**, pp. 359–363.
3. Aberg, S., Rychlik, I. and Leadbetter, M.R. (2008). Palm distributions of wave characteristics in encountering seas. *Ann. Appl. Probab.* **18**, pp. 1059–1084.
4. Azaïs, J.M. and Wschebor, M. (2009). *Level sets and extrema of random processes and fields.* John Wiley & Sons, Hoboken.
5. Bolin, D. and Lindgren, F. (2009a). Wavelet Markov approximatinos as efficient alternatives to tapering and convolution fields. *Preprints in Mathematical Sciences 2009:13*, Lund University.
6. Bolin, D. and Lindgren, F. (2009b). Spatial stochastic models generated by nested stochastic partial differential equations. *Preprints in Mathematical Sciences 2009:14*, Lund University.
7. Fouques, S., Krogstad, H.E. and Myrhaug, D. (2006). A second order Lagrangian model for irregular ocean waves. *Trans. of the ASME, J. Offshore Mechanics and Arctic Engineering*, **128**, pp. 177–183.
8. Gjøsund, S.H. (2003). A Lagrangian model for irregular waves and wave kinematics. *Trans. of the ASME, J. Offshore Mechanics and Arctic Engineering*, **125**, pp. 94–102.
9. Leadbetter, M.R., Lindgren, G. and Rootzén, H. (1983). *Extremes and related properties of random sequences and processes.* Springer-Verlag, New York.
10. Lindgren, F. and Rue, H. (2008). On the second-order random walk model for irregular locations, *Scandinavian Journal of Statistics*, **35**, pp. 691-700.
11. Lindgren, G. (2006). Slepian models for the stochastic shape of individual Lagrange sea waves. *Adv. Appl. Prob.* **38**, pp. 430–450.
12. Lindgren, G. (2009). Exact asymmetric slope distributions in stochastic Gauss-Lagrange ocean waves. *Applied Ocean Research*, **31**, pp. 65–73.
13. Lindgren, G. and Aberg, S. (2008). First order stochastic Lagrange models for front-back asymmetric ocean waves. *J. Offshore Mechanics and Arctic Engineering*, 131 (2009) p. 031602-1 – 031602-8.
14. Lindgren, G. and Broberg, K.B. (2004). Cycle range distributions for Gaussian processes – exact and approximative results. *Extremes*, 7, (2004) 69–89.
15. Lindgren, F., Lindström, J. and Rue, H. (2010). An explicit link between Gaussian fields and Gaussian Markov random fields: The SPDE approach. Preprint Statistics No. 5/2010. Norwegian University of Science and Technology, Trondheim, Norway.
16. Miche, M. (1944). Mouvements ondulatoires de la mer on profondeur constante ou décroissante. Forme limit de la houle lors de son déferlement. Application aux digues marines. *Ann. Ponts Chassées*, **114**, pp. 25–78.
17. Socquet-Juglard, H., Dysthe, K.B., Trulsen, K., Fouques, S., Liu, J. and Krogstad, H. (2004). Spatial extremes, shape of large waves, and Lagrangian models. In *Proc. Rogue Waves, Brest, 2004*. Available at http://www.ifremer.fr/web-com/stw2004/rw/fullpapers/krogstad.pdf.
18. WAFO-group, (2007). *WAFO – A Matlab Toolbox for Analysis of Random Waves and Loads - A Tutorial*, Mathematical Statistics, Center for Mathematical Sciences, Lund University, Sweden. URL http://www.maths.lth.se/matstat/wafo.